Observation of sequential spin flips in quantum rings

E. Räsänen,[1,*] A. Mühle,[2] M. Aichinger,[3] and R. J. Haug[2]
[1]*Nanoscience Center, Department of Physics, University of Jyväskylä, FI-40014 Jyväskylä, Finland*
[2]*Institut für Festkörperphysik, Leibniz Universität Hannover, Appelstr. 2, D-30167 Hannover*
[3]*Radon Institute for Computational and Applied Mathematics (RICAM), A-4040 Linz, Austria*
(Received 5 October 2011; published 21 October 2011)

We observe strong signatures of spin flips in quantum rings exposed to external magnetic fields in the Coulomb blockade regime. The signatures appear as a pattern of lines corresponding to local reduction of conductance, and they cover a large range of magnetic fields and number of electrons. The sequence of lines, as well as other features in the conductance, can be captured by many-electron calculations within density-functional theory. The calculations show that most lines in the pattern correspond to sequential spin flips between filling factors 2 and 1. We believe that the ability to probe individual spin flips provides an important step toward precise spin control in quantum ring devices.

DOI: 10.1103/PhysRevB.84.165320 PACS number(s): 73.21.La, 71.15.Mb

I. INTRODUCTION

Semiconductor quantum rings (QRs) have attracted significant interest in low-dimensional nanotechnology. QRs have potential applications in quantum information processing, especially through the Aharonov-Bohm effect,[1] that can be used to control the interference in QRs.[2] On the other hand, utilizing the Coulomb (or spin) blockade and the Kondo effect in QRs could provide a path to charge and spin control.

The experimental controllability of QRs in the Coulomb blockade regime has appeared to be more tedious than in quantum dots. For example, spin flips at filling factors $2 > \nu > 1$,[3–5] as well as signatures of fractional filling factor states[7,8] have been observed in quantum dots, but in QRs such features have not been previously seen. It is noteworthy that the spectral structure of a QR differs markedly from that of a quantum dot and it is characterized by constant level crossings as a function of the magnetic flux (see, e.g., Ref. 6).

In this paper we give clear experimental evidence of spin effects in QRs in the Coulomb blockade regime. The observed regular patterns in the conductance spectrum are shown—through extensive spin-density-functional calculations—to account for sequential spin flips at filling factors $2 > \nu > 1$. Moreover, we detect the formation of the energetically stable $\nu = 2$ state and a possibility of signals at $\nu < 1$. We can also qualitatively interpret additional features in the spectrum, e.g., occasional splittings in the conductance lines. In the following we first describe the QR device and the measurement; then present the model, theory, and computational details; and, finally, compare experiments to theory in a detailed analysis.

II. EXPERIMENT

The QR device shown in Fig. 1(a) has been fabricated from a GaAs/AlGaAs heterostructure consisting (from top to bottom) of (i) a 5-nm GaAs cap layer, (ii) 8 nm of AlGaAs, (iii) a Si-δ layer, (iv) a 20-nm-thick AlGaAs barrier, and (v) 100 nm of GaAs. The 2DEG is located between layers (iv) and (v) with an electron density of 4.3×10^{15} m^{-2} and mobility of 42.1 m^2 V^{-1} s^{-1}. The QR structure has been formed by local anodic oxidation, so the width of oxide lines is about 100 nm, and the inner and outer diameters of the QR structure are about 190 and 450 nm, respectively. The leads (source and drain) are connected to the QR through ∼150-nm-wide channels, and a voltage V_G is applied to the respective gate on the right side of the structure as shown in Fig. 1(a).

Measurements are performed by use of a standard lock-in technique. A voltage of 10 μV is applied, and the current through the system is measured in this two-terminal setup. The number of electrons in the ring is varied with the gate voltage V_G.

Figure 2 shows the measured conductance as a function of the magnetic field and V_G. The first horizontal Coulomb blockade line is observable at $V_G \sim -360$ mV. It is followed by a sequence of lines at higher voltages, indicating an increase in the number of electrons N confined in the QR. At the same time the distance between the lines decrease indicating an increase in the capacitance between the ring and the gate due to the filling up of the ring with electrons. It can be expected that the first visible Coulomb blockade lines correspond to about 10 electrons in the QR, whereas at $V_G \sim 120$ mV about 100 electrons occupy the ring.

Several distinctive features can be observed in Fig. 2. First, above the regular sequence of Coulumb-blockade lines we find signatures of Kondo conductance between the lines. This corresponds to a situation where N is unchanged but the electrons in the leads form singlet states with the unpaired electrons on the edge of the QR, leading to a high conductance. Second, at larger voltages and magnetic fields of $B > 1$ T we find a vast region of an almost constant high conductance ($G \gtrsim 1.75\ e^2/h$). Since we are measuring in a two-terminal setup, and the contact resistances to the ring are unknown, we can assume that the measured $G \gtrsim 1.75\ e^2/h$ corresponds to $G \sim 2e^2/h$ in the ring itself. This is a clear signature of the opening of the QR into the regime of ballistic transport. Third, the most peculiar large-scale feature in the conductance pattern is the ensemble of curves showing locally reduced conductance. The first lines emerge at $V_G \sim -360$ mV at low magnetic fields. They are joined by more lines for gate voltages up to -120 mV and continue up to the maximum voltage *through* the ballistic regime at higher magnetic fields. These curves are bent upward. They are observed at the highest gate voltages and at magnetic fields larger than 3 T.

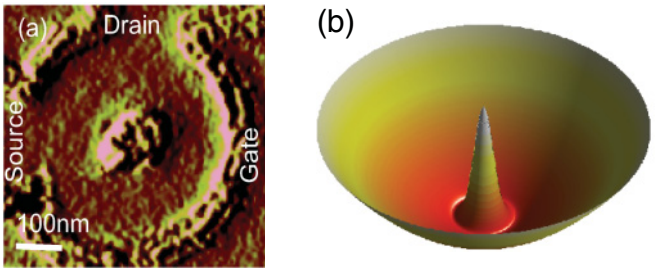

FIG. 1. (Color online) (a) Image of the quantum ring device taken with an atomic force microscope. (b) Model potential used in the calculations within spin-density-functional theory.

Occasionally the curves cross, but they are predominantly going in parallel.

III. THEORY AND MODELING

To understand these astonishing observations we have to model our QR. We apply the effective-mass approximation for electrons in GaAs with $m^* = 0.067\, m_e$ for the effective mass, $\epsilon = 12.7\,\epsilon_0$, for the dielectric constant $g^* = -0.44$ for the gyromagnetic ratio. The QR is assumed to be strictly two-dimensional (2D), so the energy spectrum lies on the lowest sub-band in the perpendicular (z) direction. The vector potential is applied in linear gauge, i.e., $\mathbf{A} = -By\,\mathbf{e}_x$. The model potential for the QR confined in the xy plane is given by $V_{\rm ext}(r) = m^*\omega_0^2 r^2/2 + V_0 \exp(-r^2/d^2)$, with $\hbar\omega_0 = 5$ meV, $V_0 = 200$ meV, and $d = 10$ nm. The potential is shown in Fig. 1(b). It should be noted that the QR radius resulting from the model is significantly smaller than that of the sample [Fig. 1(a)]. This is due to numerical restrictions to deal with up to ~100 electrons in the QR of the experimental size. However, we aim at qualitative understanding of the many-electron effects within the same filling-factor regime determined by the average number of flux quanta per electron.

We apply spin-density-functional theory (SDFT) to calculate the ground states for QRs containing up to 30 electrons. An external vector potential is included in the Kohn-Sham equation to account for the perpendicular magnetic field. The exchange and correlation are dealt with the 2D local spin-density approximation (2D-LSDA), where we use the parametrization of Attaccalite *et al.*[9] for the correlation part. Previous SDFT calculations for both quantum dots[7] and QRs[10] have confirmed the good accuracy of the 2D-LSDA calculations in comparison with numerically exact methods. It should be also noted that the QR width is sufficiently large to avoid the breaking of the 2D-LSDA in the quasi-1D limit.[11] In the numerical solution of the Kohn-Sham equations we apply a response-functional formalism to reduce the number of self-consistency loops, as well as a fourth-order factorization of the evolution operator in the eigenvalue problem.[6]

IV. COMPUTATIONAL RESULTS

The suppression of the conductance in the nearly ballistic regime results from changes in the (many-electron) states that leave signatures in the addition energies as a function of the magnetic field. The addition energies correspond to differences in the chemical potentials for successive electron

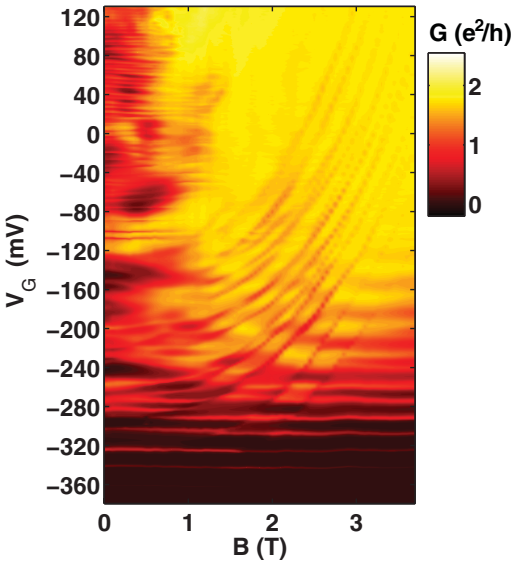

FIG. 2. (Color online) Measured conductance in the quantum-ring device over a wide range of gate voltages and magnetic fields.

numbers, i.e., $\Delta(N) = \mu(N+1) - \mu(N) = E(N+1) - 2E(N) + E(N-1)$. Here $E(N)$ is the ground-state energy obtained by performing a set of SDFT calculations for different states with spin S and choosing the state with the lowest energy.

Figure 3 shows the calculated addition energies up to $N = 30$. A rich pattern of features can be observed at different B and N. Many of these features have been theoretically investigated in, e.g., Refs. 6 and 12, with, however, a focus on the low-N regime. It can be immediately seen that at high magnetic fields the addition energy pattern shows a similar sequence of lines as the measured conductance in Fig. 2. As shown explicitly below, the line pattern corresponds to sequential spin flips at filling factors $2 > \nu > 1$. Moreover, in accordance with the experiment, there are several line crossings, pronouncedly at

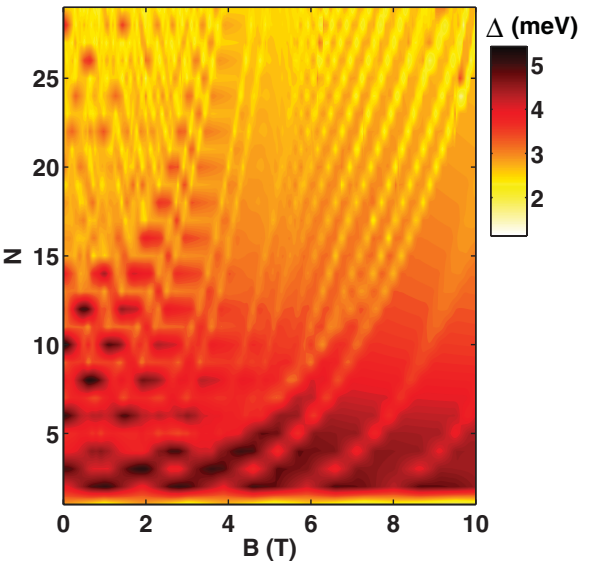

FIG. 3. (Color online) Addition energies calculated with spin-density-functional theory.

$N \sim 10 \ldots 15$. They result from the increasing degeneracy of single-electron (or here Kohn-Sham) states as a function of N, especially in the vicinity of the $\nu = 2$ state. Thus, we may see a splitting of a particular ground-state sequence into two, leading to a separation between the curves in the spectrum.

The two rightmost curves in Fig. 3 at small N and $B \sim 6 \ldots 10$ T correspond to changes in the ground state in the fully polarized regime at $\nu < 1$ attributed to vortex formation in the QR.[6] These curves are separated further from each other than the spin-flip lines. In fact, the rightmost lines in the experimental spectrum (Fig. 2) show similar tendency. To analyze this in detail, we can estimate the filling factor from $\nu = N/N_\Phi$, where $N_\Phi = \Phi/\Phi_0$ is the number of flux quanta and $\Phi_0 = h/e$. Assuming that the first few Coulomb blockade lines in the experimental spectrum correspond to $N \sim 10$, and that the QR radius is $R \sim 100$ nm [Fig. 1(a)], the onset of the polarized regime at $\nu = 1$ should lie at $\sim$1.3 T. Therefore, it is possible that the rightmost signals across the Coulomb blockade lines in Fig. 2 are located at $\nu < 1$, although we cannot confirm this assessment due to the uncertainty in N and particularly in the precise QR radius.

In Fig. 4 the experimental and theoretical electron addition spectra are compared in detail by taking cross sections, respectively, at $V_G = -40, 0, 40, 80$ mV and $N = 20, 23, 26, 29$. Several similar features can be observed, and in the following we compare them in three domains separated by dashed lines in Fig. 4. We start with high magnetic fields, where the spin-flip regime appears as a pattern of relatively regular peaks. In the theoretical result the peak amplitude increases as a function of B, which is due to the higher excitation energy at each spin flip: the spin degeneracy is lifted from lower and lower levels when B increases (toward the lowermost level which dissolves last when $\nu = 1$). In the experiment, on the other hand, the peak amplitude has an opposite tendency to decrease as a function of B. We expect this to be due to the fact that high magnetic fields support ballistic transport which dominates the spectrum as a whole (Fig. 2).

As shown in Fig. 4, the spin-flip regime is preceded by a relatively flat plateau region in both experiment and theory. This is due to the high stability of the system in terms of energy at $\nu \sim 2$ as the lowest Landau level gets populated and the spin polarization is (close to) zero. Similar stability of the $\nu = 2$ state in quantum dots has been experimentally confirmed several times[4,13] and theoretically analyzed in, e.g., Ref. 7 and for QRs in Ref. 10. At even smaller magnetic fields we find strong bumps in both experimental and theoretical spectra. They correspond to the depopulation of the second-lowest Landau level. It should be noted that the fine structure seen in the calculations is washed out in the experimental spectrum due to the ballistic threshold discussed above. In the experimental data we see this transition to ballistic transport directly in the strong increase of the conductance at small magnetic fields. Therefore, by comparing the experimental data with the theoretical results we are able to identify a number of interesting features, especially the spin flips appearing in a regular fashion.

To further understand the spin structures appearing here, Fig. 5 shows the ground-state spins for QRs containing 18, 26, and 30 electrons, respectively, as a function of the magnetic field. In low fields at $\nu > 2$ the spins alternate between $S = 0, 1, 2$ due to the partial polarization of electrons in the few highest levels. This is mainly an exchange effect reminiscent of Hund's rule in atoms. At $\nu < 2$ instead, the sequential spin flips on the lowest Landau level are clear. The underlying physical effect behind the behavior is still the electronic exchange as the differences in the energy levels decrease as a function of B. In addition, the Zeeman effect, i.e., the energy difference between levels of different spin, which is linear in B, has an increasing role.

At certain magnetic fields we find partial depolarization marked by circles in Fig. 5. They result from the complex

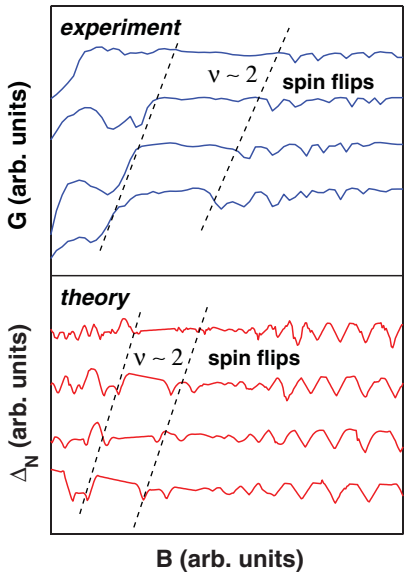

FIG. 4. (Color online) Experimental (upper panel) and theoretical (lower panel) cross sections of the electron addition spectra, respectively.

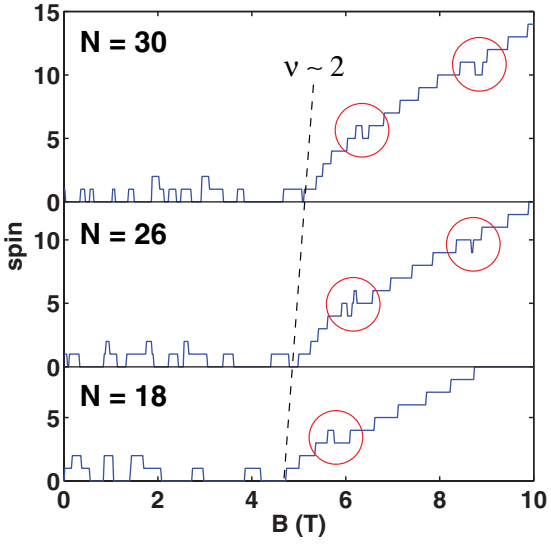

FIG. 5. (Color online) Calculated ground-state spins in quantum rings containing 18, 26, and 30 electrons, respectively, as a function of the magnetic field. The circles mark the regimes of local depolarization (see text).

arrangement of the highest occupied (Kohn-Sham) energy levels that break the regularity of the spin flips discussed above. Although these features appear systematically with respect to N, they leave no detectable signal in the calculated addition energy and are difficult to be seen also in the experimental transport data. This is due to the fact that at those points there are several many-electron states with almost the same total energy, including the ones that would show a regularly increasing spin sequence.

V. SUMMARY

To summarize, we have measured the conductance spectrum of quantum rings in the Coulomb blockade regime with high sensitivity, which has led to an observation of unexpected features as a function of the magnetic field. To analyze the experimental data, we have performed spin-density-functional calculations up to 30 electrons and found a convincing qualitative agreement with the measured features. In particular, we have attributed the regular pattern of curves to sequential spin flips between filling factors $2 > \nu > 1$. In addition, we have experimentally verified the previously predicted high stability of the $\nu = 2$ state and analyzed the unexpected features in the spectrum such as the (dis-)connection of lines. We believe that the demonstrated ability to probe individual spin flips in relatively large quantum rings provides an important step toward precise spin control in quantum-ring devices.

ACKNOWLEDGMENTS

We acknowledge the sample growth and processing by W. Wegscheider, M. Bichler, U. Keyser, and S. Borck. This work has been supported by the cluster QUEST within the German Excellence Initiative (A.M. and R.J.H.) and by the Academy of Finland (E.R.).

*erasanen@jyu.fi

[1] Y. Aharonov and D. Bohm, Phys. Rev. **115**, 485 (1959); **123**, 1511 (1961).

[2] For experimental results, see, e.g., A. Fuhrer, S. Lüscher, T. Ihn, T. Heinzel, K. Ensslin, W. Wegscheider, and M. Bichler, Nature **413**, 822 (2001); U. F. Keyser, C. Fühner, S. Borck, R. J. Haug, M. Bichler, G. Abstreiter, and W. Wegscheider, Phys. Rev. Lett. **90**, 196601 (2003); D.-I. Chang, G. L. Khym, K. Kang, Y. Chung, H.-J. Lee, M. Seo, M. Heiblum, D. Mahalu, and V. Umansky, Nat. Phys. **4**, 205 (2008).

[3] P. L. McEuen, E. B. Foxman, J. Kinaret, U. Meirav, and M. A. Kastner, N. S. Wingreen, and S. J. Wind, Phys. Rev. B **45**, 11419 (1992).

[4] M. Ciorga, A. S. Sachrajda, P. Hawrylak, C. Gould, P. Zawadzki, S. Jullian, Y. Feng, and Z. Wasilewski, Phys. Rev. B **61**, R16315 (2000).

[5] C. Gould, P. Hawrylak, A. Sachrajda, Y. Feng, P. Zawadzki, and Z. Wasilewski, Physica E **6**, 461 (2000).

[6] M. Aichinger, S. A. Chin, E. Krotscheck, and E. Räsänen, Phys. Rev. B **73**, 195310 (2006).

[7] E. Räsänen, H. Saarikoski, A. Harju, M. Ciorga, and A. S. Sachrajda, Phys. Rev. B **77**, 041302(R) (2008).

[8] M. C. Rogge, E. Räsänen, and R. J. Haug, Phys. Rev. Lett. **105**, 046802 (2010).

[9] C. Attaccalite, S. Moroni, P. Gori-Giorgi, and G. B. Bachelet, Phys. Rev. Lett. **88**, 256601 (2002).

[10] E. Räsänen and M. Aichinger, J. Phys. Condens. Matter **21**, 025301 (2009).

[11] E. Räsänen, S. Pittalis, C. R. Proetto, and E. K. U. Gross, Phys. Rev. B **79**, 121305(R) (2009).

[12] A. Emperador, M. Pi, M. Barranco, and E. Lipparini, Phys. Rev. B **64**, 155304 (2001).

[13] M. C. Rogge, C. Fühner, and R. J. Haug, Phys. Rev. Lett. **97**, 176801 (2006).